IOPscience iopscience.iop.org

Home Search Collections Journals About Contact us My IOPscience

Bose-Einstein condensation in a pure Ioffe-Pritchard field configuration

This content has been downloaded from IOPscience. Please scroll down to see the full text.

1998 Europhys. Lett. 41 1

(http://iopscience.iop.org/0295-5075/41/1/001)

View the table of contents for this issue, or go to the journal homepage for more

Download details:

IP Address: 129.93.16.3
This content was downloaded on 23/08/2015 at 19:55

Please note that terms and conditions apply.

EUROPHYSICS LETTERS 1 January 1998

Europhys. Lett., **41** (1), pp. 1-6 (1998)

Bose-Einstein condensation in a pure Ioffe-Pritchard field configuration

U. Ernst, A. Marte(*), F. Schreck, J. Schuster and G. Rempe

Fakultät für Physik, Universität Konstanz, Fach M701, D-78457 Konstanz, Germany

(received 22 October 1997; accepted in final form 20 November 1997)

PACS. 03.75.Fi – Phase coherent atomic ensemble.
PACS. 05.30.Jp – Boson systems.
PACS. 32.80.Pj – Optical cooling of atoms; trapping.

Abstract. – A glass-cell apparatus and a dc magnetic trap with radial gradient of 275 G/cm and axial curvature of 365 G/cm^2 were used to capture and evaporatively cool rubidium 87 atoms. Below a critical temperature of 550 nK, Bose-Einstein condensation was observed with 10^6 atoms in the trap. Pure condensates with more than 10^5 atoms and peak densities exceeding 4×10^{14}cm^{-3} were produced.

One of the most fascinating predictions of quantum-statistical mechanics is that of a phase transition in an ideal gas of identical bosons when the thermal de Broglie wavelength exceeds the mean spacing between the particles. Under such conditions, a macroscopic number of bosons occupies the lowest energy state [1], [2]. This phenomenon is termed Bose-Einstein condensation (BEC) and has been observed in dilute atomic gases in the pioneering experiments of 1995 [3]-[5]. The gases were cooled to ultra-low temperatures by a combination of laser cooling [6] and evaporative cooling [7] techniques. The required densities were achieved in magnetic traps with two different field configurations: One employs a 3D magnetic quadrupole field in combination with either a rotating field, the TOP trap [3], or a blue-detuned laser beam propagating through the trap center [5], in order to suppress spin-flip losses in a region where the magnetic field is close to zero. The TOP trap was also used in recent BEC experiments [8], [9]. The other approach uses variations of the Ioffe-Pritchard configuration [10], which employs purely dc magnetic fields with a non-zero field in the trap center, like the permanent magnet [4], the clover leaf [11], [12] and the baseball trap [13]. The present paper reports on BEC of ^{87}Rb atoms trapped in a dc magnetic field generated by currents through a clip-like coil for radial confinement and two pinch coils for axial confinement. This configuration has not been used in previous BEC experiments and offers the distinctive advantage that condensates with purely 2D confinement along the radial direction can be studied.

(*) Present address: Integrated Systems Laboratory, Swiss Federal Institute of Technology, Zürich, Switzerland.

© EDP Sciences

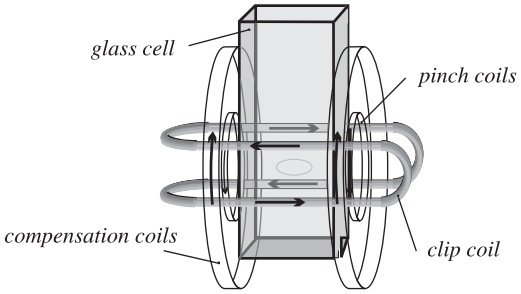

Fig. 1. – Scheme of the magnetic trap.

An important condition for runaway evaporative cooling is a high density of trapped atoms. This can be achieved in a tightly confining magnetic trap, as characterized by high oscillation frequencies of the atoms in the trapping potential. The large mass of Rb requires magnetic fields with high gradients and curvature. This condition is fullfilled in the trap shown in fig. 1. It consists of 5 coils made of water-cooled copper tubes. One coil has the shape of a clip with size 13 cm×4 cm×4 cm. It generates a two-dimensional quadrupole field for radial confinement. A current of 575 A through the 6 turns produces a gradient of 275 G/cm. We emphasize that the curved ends of the long clip-like coil produce only a small homogeneous field with negligible axial curvature in the center of the trap. Two plane pinch coils with inner radius 1.4 cm and separation 4.5 cm are mounted symmetrically inside the clip coil. They create a bottle field which confines the atoms along the axial direction. A field curvature of 365 G/cm^2 is achieved with a current of 455 A through 6 turns. An additional pair of Helmholtz coils, separated by 5.8 cm and mounted outside the clip coil, serves to compensate the bias field in the center of the trap. The currents can be turned on and off with a slew rate of 10^6 A/s. The trapping potential can be adjusted by setting the currents through the 5 coils. This allows to realize three different potential shapes, either a 3D harmonic potential with spherical symmetry, or a 3D potential with axial symmetry, or a potential with 2D confinement but flat along the horizontal axis. The coil arrangement provides good optical access along the axial and two orthogonal radial directions.

The experimental setup was specially designed for the BEC experiment and allows to collect many atoms under good vacuum conditions, an essential requirement for evaporative cooling. The vacuum system consists of two chambers connected by a 20 cm long and 1 cm wide vertical tube. The upper chamber houses a vapour-cell magneto-optical trap (MOT) for ^{87}Rb atoms with two horizontal retro-reflected laser beams and two independent vertical beams. This MOT acts as a source of atoms for the second MOT located in the lower chamber [14]. The lower MOT is operated in a 3 cm×3 cm×7 cm glass cell at a background pressure of 10^{-11} mbar. It shares the vertical trapping laser beams with the upper MOT, but uses four independent horizontal laser beams. Light at the trapping frequency is provided by a grating-stabilized diode laser [15] tuned to the atomic cycling transition $5S_{1/2}F = 2 - 5P_{3/2}F = 3$. Its output power is amplified with two independent 40 mW injection-locked laser diodes. One of these two lasers produces the light for both MOTs, while the other laser provides additional light beams for controlling and detecting the atoms at various stages of the experiment. A second grating-stabilized diode laser is tuned to the atomic transition $5S_{1/2}F = 1 - 5P_{3/2}F = 2$ and generates repumping light for both MOTs.

The first step in the experiment is to load the upper MOT for 500 ms. Transfer of atoms from the upper MOT into the lower MOT is achieved by pushing them downwards with a 1 ms light pulse resonant to the atom's cycling transition. Previously, the trapping force of the upper MOT is removed by switching off the magnetic quadrupole field. The upper MOT's repumping light is turned off after 500 μs, and an additional laser beam resonant with the $5S_{1/2}F = 2 - 5P_{3/2}F = 2$ transition is turned on at this moment. Thus, atoms are now pumped into the state $5S_{1/2}F = 1$, where they are not affected by the push and trapping beams due to the large hyperfine splitting of 6.8 GHz. This avoids heating during the 40 ms long transfer time, while the atoms are moving along the two vertical trapping beams with a velocity of about 10 m/s, before being recaptured in the lower MOT. The single shot transfer efficiency is estimated to be close to 50%. By repeating the loading cycle up to 100 times with a repetition rate of 2 Hz, more than 10^9 atoms could be collected in the lower MOT. The number of atoms was determined by monitoring the spatial absorption profile as a function of laser frequency. The lifetime of the lower MOT was measured to be 70 s.

After loading, the cloud of atoms is compressed [16] by increasing the magnetic-field gradient and the detuning of the trapping light, and by decreasing the intensities of the trapping beams within 80 ms. As a result, the size of the atomic cloud decreases from 3.5 mm to 2.5 mm (FWHM) and its shape becomes more spherical. To achieve a sub-Doppler temperature of ≈ 40 μK, the magnetic quadrupole field is turned off and polarisation-gradient cooling is applied for 5 ms. The atoms are then optically pumped within 150 μs into the weak-field seeking state $5S_{1/2}F = 2$, $m_F = 2$ of the upper ground state hyperfine structure manifold. Note that this state is dark for the circular polarized pumping light resonant with the transition $5S_{1/2}F = 2 - 5P_{3/2}F = 2$. During optical pumping the repumping light is on and an additional 3 G guiding field is applied along the quantization direction, which is defined by the symmetry axis of the magnetic trap.

The initial magnetic potential has to be mode-matched to the shape of the atom cloud after molasses cooling. Hence, the trapping potential is spherically symmetric with an atomic oscillation frequency of 10 Hz. In addition, the spatial position of the MOT is fine-tuned with respect to the fixed minimum of the magnetic trapping potential by means of 3 orthogonal coils which are operated in series with the 2 MOT coils. This helps to compensate the effect of gravity, which shifts the center of the shallow magnetic trap. After transfer, this would transform gravitational energy into heat during the thermalization process. The final temperature of the magnetically trapped atoms is measured to be 70 μK. The transfer efficiency is about 70%. Next, the atomic cloud is adiabatically compressed by continuously increasing the currents through the 5 coils within 6 s. After compression, the bias field has a magnitude of 1.5 G as determined from rf-induced spin-flip losses (see below). From this value and the trap geometry the oscillation frequencies are calculated to be $\omega_\parallel = 2\pi\times 24$ Hz and $\omega_\perp = 2\pi\times 280$ Hz. Small trap frequencies ($\omega_\parallel, \omega_\perp \leq 2\pi\times 24$ Hz) were also measured by monitoring the oscillation of an atomic cloud in the trap. We find good agreement between measured and calculated frequencies within $\pm 2\pi\times 0.5$ Hz.

Finally, evaporative cooling is applied to increase the cloud's phase-space density from its initial value of 5×10^{-8}. A rf magnetic field is produced by two coils on two opposite sides of the glass cell, with the rf field perpendicular to the magnetic field in the center of the trap. The rf frequency is continuously tuned from a maximum initial value of 50 MHz to a final value close to 1.4 MHz within 20 s. The evaporation process was optimized by measuring the increase of phase-space density per particle loss. We have initially tested this strategy in numerical simulations of the cooling process. At the end, the atomic cloud was allowed to thermalize for 100 ms, with the rf scan off.

The atomic cloud is probed by time-of-flight absorption imaging for variable delay times

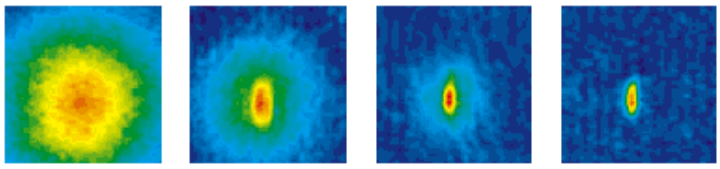

Fig. 2. – False-colour absorption images obtained 26 ms after releasing the atoms from the magnetic trap. The pictures a), b) and c) are taken at temperatures of 1.2 μK, 310 nK, and 170 nK, respectively. Picture d) displays a pure condensate without a discernible fraction of thermal atoms.

after suddenly switching off the trap. A 150 μs light pulse resonant with the atomic cycling transition is used. The probe beam propagates horizontally in the radial plane of the trap. One achromatic lens images the atomic cloud onto a standard CCD-Chip. An 8-bit frame grabber is used to digitize the data. After sufficiently long expansion times, the thermal cloud is spherically symmetric and the temperature can be determined from the size of the cloud. Figure 2 shows false-colour images obtained 26 ms after releasing the atoms from the trap. The size of the images is 0.75 mm by 0.75 mm with a resolution of 10 μm per pixel. Picture a) displays a pure thermal cloud with a temperature of 1.2 μK. Pictures b) and c) are obtained at 310 nK and 170 nK, respectively. An elliptic core in the center of the thermal cloud is clearly visible. The size of the elliptic core is found to be nearly independent of temperature. With further evaporation the thermal cloud vanishes, until — as shown in picture d) — an almost pure condensate is left. The ellipticity is due to the anisotropic expansion of the condensate, as expected for an asymmetric trapping potential [3].

The sudden appearence of the BEC phase transition is even more impressive by looking at horizontal sections through the pictures displayed in fig. 2. For decreasing temperatures, a bimodal distribution with a decreasing fraction of thermal atoms is clearly visible, as shown in fig. 3. The distribution of thermal atoms is Gaussian, as can be seen from the dashed curve which represents a fit with temperature as an adjustable parameter. The distribution of condensed atoms, however, is not Gaussian, but is determined by the harmonic trapping potential. In the Thomas-Fermi approximation, the density distribution is an inverted parabola [17]. This is displayed in fig. 4a), where a vertical section through picture 2d) is plotted. The dashed curve represents the result of a fit using a parabolic density distribution integrated

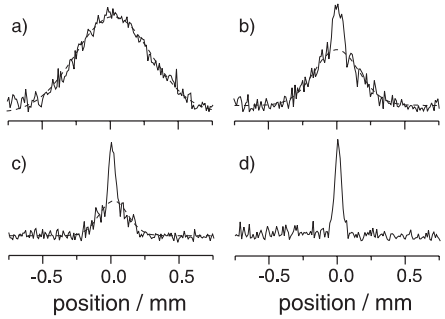

Fig. 3. – Horizontal sections through pictures a)-d) of fig. 2.

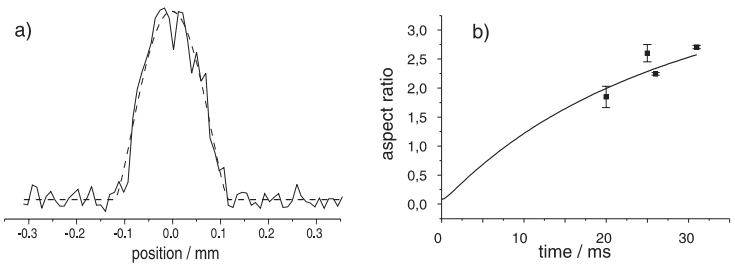

Fig. 4. – a) Radial density profile of the condensate after a 26 ms long free expansion featuring its parabolic shape (dashed curve). b) Aspect ratio of the freely expanding condensate *vs.* time, with the solid curve taken from [17].

along the propagation direction of the probe beam. In addition to the bimodal distribution discussed above, the good agreement between the measured shape and the fitted curve provides strong evidence for the existence of a core of condensed atoms.

For an asymmetric trapping potential the aspect ratio $\epsilon(t)$ of the observed ellipse during the free expansion is time dependent and only determined by the trap oscillation frequencies $\omega_\parallel$ and $\omega_\perp$. Figure 4b) displays the measured $\epsilon(t)$ for 4 different expansion times $t = 20\,\mathrm{ms}$, 25 ms, 26 ms and 31 ms, with uncertainty due to small fluctuations of the transversal trap frequency and probe beam parameter. The theoretical curve taken from [17] agrees well with the experimental data. Note that in our experiment the long axis of the density distribution displays the condensate's momentum distribution, while the short axis still resembles its position distribution.

The critical temperature (T_c) for BEC in our trap can be obtained from a series of data like those shown in fig. 3. We find $500\,\mathrm{nK} < T_\mathrm{c} < 600\,\mathrm{nK}$. The total number N of thermal atoms at T_c is estimated from the absorption signal as described above, and by extrapolating the optimized phase-space density to temperatures close to T_c. Both techniques give the same result, $N = 10^6$. The observed T_c is in good agreement with the expected transition temperature, $k_\mathrm{B}T_\mathrm{c} = \hbar\bar{\omega}(N/1.202)^{1/3} = k_\mathrm{B} \times 550\,\mathrm{nK}$, where $\bar{\omega} = (\omega_\parallel\omega_\perp\omega_\perp)^{1/3} = 2\pi\times 123$ Hz.

For more than a few thousand condensed atoms, N_0, the condensate has a mean field energy $U = 2\mu/7$. Here $\mu = n_0 u$ denotes the chemical potential and $n_0 = 0.118(N_0 m^3\bar{\omega}^3/\hbar^3 a^{3/2})^{2/5}$ is the peak density of the condensed atoms with mass m, s-wave scattering length $a = 5.3$nm and two-body pseudopotential $u = 4\pi\hbar^2 a/m$ [18]. In our case, $U = k_\mathrm{B} \times 40\,\mathrm{nK}$, which is significantly larger than the trap's zero-point energy of $k_\mathrm{B} \times 14\,\mathrm{nK}$. The mean-field energy gives rise to a mainly radial expansion of the condensate after suddenly turning off the trap. A rough estimate for N_0 can therefore be obtained from the radial size of the condensate after a fixed time delay, *e.g.*, 240 μm after 26 ms as in fig. 4a). The result is $N_0 = 10^5$ for the case of the pure condensate. This justifies the use of the Thomas-Fermi approximation. The chemical potential is $k_\mathrm{B} \times 140\,\mathrm{nK}$, and the peak density is $n_0 = 4 \times 10^{14}\,\mathrm{cm}^{-3}$. For $N_0 = 10^5$ atoms, the full width of the condensate in the magnetic trap is estimated to be 5 μm in the radial and 60 μm in the axial direction.

In conclusion, we have achieved BEC of Rb atoms in a dc magnetic trap, which allows us to study a condensate released along the axial direction only. This advantage is not shared by the traps used in previous BEC experiments, and provides 2D confinement for 1D nonlinear atom optics [19], [20]. In combination with, *e.g.*, far-detuned light sheets, this would also make it possible to build a Fabry-Perot–type interferometer [21] for condensed atoms [22], or to study step-wise condensation [23] in a highly anisotropic trap with weak axial confinement.

***

The authors thank S. KUNZE for writing part of the software, W. PETRICH for discussions, and B. SANG for help in constructing the high-current switch. We greatfully acknowledge financial support by the Optikzentrum Konstanz and the Deutsche Forschungsgemeinschaft.

REFERENCES

[1] BOSE S. N., *Z. Phys.*, **26** (1924) 178.
[2] EINSTEIN A., *Sitzber. Kgl. Preuss. Akad. Wiss.*, (1925) 3.
[3] ANDERSON M. H. *et al.*, *Science*, **269** (1995) 198.
[4] BRADLEY C. C. *et al.*, *Phys. Rev. Lett.*, **75** (1995) 1687.
[5] DAVIS K. B. *et al.*, *Phys. Rev. Lett.*, **75** (1995) 3969.
[6] ARIMONDO E., PHILLIPS W. D. and STRUMIA F. (Editors), *Laser Manipulation of Atoms and Ions, Proceedings of the International School of Physics "Enrico Fermi", Varenna*, Course CXVIII (North Holland, Amsterdam) 1991.
[7] KETTERLE W. and VAN DRUTEN N. J., *Advances in Atomic, Molecular and Optical Physics*, edited by B. BEDERSEN and H. WALTHER, Vol. **37** (Academic Press, San Diego) (1996) p. 181.
[8] HEINZEN D., talk at the European Research Conference on Bose-Einstein-Condensation, Castelvecchio Pascoli, Italy, 1997.
[9] KASEVICH M., talk at the *IV Workshop Optics and Interferometry with Atoms*, St John's College, Oxford, 21st-23rd July 1997.
[10] PRITCHARD D. E., *Phys. Rev. Lett.*, **51** (1983) 1336.
[11] MEWES M.-O. *et al.*, *Phys. Rev. Lett.*, **77** (1996) 416.
[12] HAU L., in *Photonic, Electronic, and Atomic Collisions, Proceedings of the XX ICPEAC, Vienna, Austria, 1997*, edited by F. AUMAYR and H. P. WINTER (World Scientific) 1998.
[13] MYATT C. J. *et al.*, *Phys. Rev. Lett.*, **78** (1997) 586.
[14] MYATT C. J. *et al.*, *Opt. Lett.*, **21** (1996) 290.
[15] KUNZE S. *et al.*, *Opt. Commun.*, **128** (1996) 269.
[16] PETRICH W. *et al.*, *J. Opt. Soc. Am. B*, **11** (1994) 1332.
[17] CASTIN Y. and DUM R., *Phys. Rev. Lett.*, **77** (1996) 5315.
[18] See, *e.g.*, the recent review by PARKINS S. and WALLS D. F., submitted for publication to *Phys. Rep.*, and references therein.
[19] LENZ G. *et al.*, *Phys. Rev. Lett.*, **71** (1993) 3271.
[20] ZHANG W. *et al.*, *Phys. Rev. Lett.*, **72** (1994) 60.
[21] WILKENS W. *et al.*, *Phys. Rev. A*, **47** (1993) 2366.
[22] GUZMAN A. M. *et al.*, *Phys. Rev. A*, **53** (1996) 977.
[23] VAN DRUTEN N. J. and KETTERLE W., *Phys. Rev. Lett.*, **79** (1997) 549.